Torsion balances with fibres of zero length

Speake, Clive; Collins, Chris

DOI:
10.1016/j.physleta.2018.02.015

Citation for published version (Harvard):
Speake, C & Collins, C 2018, 'Torsion balances with fibres of zero length', *Physics Letters A*, vol. 382, no. 16, pp. 1069-1074. https://doi.org/10.1016/j.physleta.2018.02.015

Physics Letters A 382 (2018) 1069–1074

Contents lists available at ScienceDirect

Physics Letters A

www.elsevier.com/locate/pla

Torsion balances with fibres of zero length

Clive C. Speake *, Christopher J. Collins

School of Physics and Astronomy, Institute of Gravitational Wave Astronomy, University of Birmingham, Edgbaston, Birmingham B15 2TT, UK

ARTICLE INFO

Article history:
Received 17 November 2017
Received in revised form 30 January 2018
Accepted 9 February 2018
Available online 21 February 2018
Communicated by M.G.A. Paris

Keywords:
Torsion balance
Gravity tests at short-ranges
Superconducting suspensions
Electrostatic suspensions

ABSTRACT

Torsion balances have good immunity to tilt and low rotational stiffness. However precise control of the position of the suspended torsion 'bob' is difficult in the presence of ground vibrations and tilt and this is a limiting factor in applications where Casimir forces or putative non-Newtonian short-range forces are being measured. We describe how the desirable characteristics of torsion balances can be reproduced in a rigid body that is suspended using applied forces rather than a torsion fibre. The suspension system can then provide a more precise control of the degrees of freedom of the suspended body. We apply these ideas to a superconducting levitated torsion balance, developed by the authors, and a generic electrostatic suspension. We present results of preliminary experiments that provide support for our analyses.

1. Introduction

The torsion balance has been the work-horse of many areas of physics and engineering since the time of Cavendish [3,5]. The advantages associated with a state of the art Cavendish torsion balance are well understood and appreciated: measurements of torques can be made without the influence of Earth's gravity; fibres can be easily manufactured that give very small torsional stiffness and this minimises the problem of noise associated with the sensor that detects the rotational motion; finally torsion balances can be made so that, to a good approximation, horizontal acceleration or tilt of the laboratory does not couple to their rotation. As a result of these attributes the torsion balance has been used with great success to test the principle of weak equivalence and the inverse square law of gravitation [15]. However the classic torsion balance does have its drawbacks: its dynamics are complex as the suspended object (the bob) is essentially suspended as a simple pendulum that can swing in the presence of ground vibrations that accelerate the attachment point of the fibre. This makes the precise control of the linear displacements of the bob difficult. Ground tilt in a typical laboratory is of the order of a few μrad and the displacement of the bob attached to the end of a fibre of a few 10's of cm in length can make measurements of forces whose range is less than a few μm problematic [10]. There is residual tilt coupling due to the asymmetry of the fibre and, therefore, most torsion balances convert ground tilt into rotation about the torsion balance fibre axis [13,1]. The question arises as to whether there could be devices that can equal the performance of the Cavendish balance in terms of their signal to noise for torque measurement, have low sensitivity to ground tilt, but have more controllable dynamics. Many attempts have been made at dispensing with the standard torsion fibre. For example there have been: superconducting gradiometers [4] and torsion balances [6]; room temperature magnetic suspensions [9]; fluid suspensions [8] and electrostatic suspensions [16]. Nevertheless our knowledge of weak forces with ranges larger than about 50 μm is still dominated by a device that was devised more than 200 years ago.

The goal of the work described here picks up from the instrument developments of reference [6] and [16] (see also [7]) where the fibre is absent. We refer to these devices as torsion balances with 'fibres of zero length'. We aim to realise post-Cavendish torsion balances that have simple dynamics such that surfaces, that provide the source and test bodies for short range forces, can be accurately maintained in close proximity but still have the desirable properties of the Cavendish torsion balance. Such a development would potentially allow more accurate measurement of forces of shorter range than 50 μm and provide a more sensitive device than atomic force microscopes (see [11]) that are currently commonly used in this regime.

We present a scheme for tuning the dynamics of a suspended object in order to decouple its rotational motion from translational accelerations and also to tune one or more of its rotational modes to give a low stiffness. We will consider a general case of a mechanically rigid object (i.e. with no internal degrees of freedom) suspended by some combination of actuators relative to some rigid structure. The actuators provide forces and stiffnesses and could be magnetic, electrostatic, air pressure actuators, mechanical springs, or some combination thereof. The forces provided by the actuators

* Corresponding author.
E-mail address: c.c.speake@bham.ac.uk (C.C. Speake).

https://doi.org/10.1016/j.physleta.2018.02.015

could individually be attractive or repulsive and their equivalent springs could produce a stability or instability in the suspended object. However, the forces and their stiffnesses have to be tunable. Clearly, if the force provided by an actuator is either attractive or repulsive, it will not by itself produce an equilibrium position, either stable or unstable. Two such actuators acting in opposition can produce a stable equilibrium if the second derivative of the potential energy with respect to a particular degree of freedom is positive for both springs, and an unstable one if the second derivatives are both negative. We will specifically address the cases of superconducting diamagnetic and electrostatic suspensions. Diamagnetic superconducting suspensions can be used to suspend an object in a stable configuration. In this case, the equilibrium position will represent a minimum of the body's potential energy in the six-dimensional space of translations and rotations. The motion, for sufficiently small deviations from the equilibrium position, should be well described by a combination of up to six harmonic oscillator modes. By Earnshaw's theorem it is not possible to stably electrostatically suspend an object in three dimensions, but it may be in a stable configuration if it is mechanically constrained in one or more dimensions, and it may also be servo-controlled such that it is effectively stable below some frequency range that is characteristic of the servo system.

In the following article we analyse the general case of a levitated rigid body that is constrained by some combination of actuators relative to some rigid external structure (attached to the Earth). We refer to the levitated object as the 'float', the actuators as 'springs' and the rigid structure as the 'bearing'. We present a model for the potential energy in terms of generalised stiffnesses which constrain the float's motion relative to the bearing. We show how the stiffnesses can be defined in order to allow one of the float's rotational degrees of freedom to be decoupled from translational vibrations of the bearing. We also show, using the specific examples of an electrostatic suspension and a superconducting torsion balance, how the stiffnesses can be modified to achieve a rotational degree of freedom of low stiffness.

2. Decoupling of translational forces from the rotational mode

The low flexural rigidity of the fibre suspension of a Cavendish torsion balance is such that the centre of mass of the suspended torsion bob lies to a high accuracy directly below the axis of rotation of the balance. This means that a transverse acceleration of the laboratory (e.g. from seismic noise) acting on the suspended mass (bob) through its centre of mass (COM) will not produce a torque on the balance. In general, for an electromagnetically suspended object, there will be some offset between the COM and the point through which the suspension forces act. This leads to a coupling between translational and rotational modes. This situation is illustrated in Fig. 1.

In Fig. 1 an object, represented by the outer rectangle (but that can in principle be of an arbitrary shape), is shown in an arbitrary orientation being supported by an array of forces, with their associated stiffnesses acting at various points on the surface of the body. We can assume, for the sake of ease of conceptual understanding, that the figure is a plan view and that local gravity acts in a perpendicular direction to the page. A steady acceleration of the bearing in the plane of the page will produce a force, $\vec{F}_c$, acting at the centre of mass of the float and a reaction force $\overrightarrow{F_b}$ at a position that we will define as the centre of buoyancy of the float/bearing system. We have from Newton's third law that

$$\vec{F}_c + \vec{F}_b = 0, \tag{1}$$

and the net torque acting on the system is

$$\Gamma = \vec{r_b} \times \vec{F}_b + \vec{r_c} \times \vec{F}_c = \left(\vec{r_c} - \vec{r_b}\right) \times \vec{F}_c. \tag{2}$$

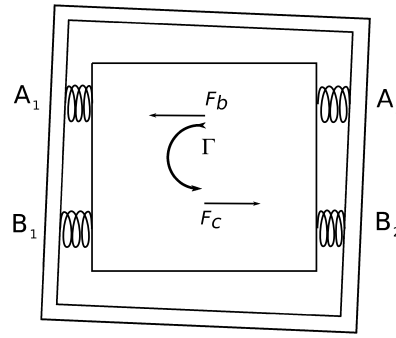

Fig. 1. A schematic diagram in two dimensions of a float (outer tilted rectangular object) that is suspended from a bearing using a combination of forces that are represented by springs in compression. A linear acceleration of the bearing creates forces F_c and F_b that act at the centre of mass of the float and centre of buoyancy of the bearing, respectively. If the centre of buoyancy is not located at the centre of mass of the float, a torque Γ is also produced. The labels for the coils are used in a discussion in Section 4.

We can equate the force acting on the float with the product of its mass, m_f, and the acceleration, $\ddot{\vec{r_0}}$, of the bearing. The coordinates of the centre of buoyancy, $\vec{r_b}$, and the centre of mass of the float, $\vec{r_c}$, can be defined with respect to a coordinate system centred on the bearing. We notice that the centre of buoyancy is the point at which a force can be applied such that it only produces a displacement of the float and not a rotation. It follows that, if the centre of mass of the float coincided with the centre of buoyancy, the float would displace but not rotate. Tuning of the centre of mass position can be achieved by adjustment of the distribution of mass, as is the case in standard mechanical beam balances where an appropriate period of oscillation can be thus achieved, for example. However here we explore the possibility of adjustment of the stiffnesses.

For a general positional configuration of the float, we can calculate the potential energy, E, stored in the ensemble of suspension springs in terms of the linear and angular displacements of the float, Δ, with respect to the bearing as

$$E = \frac{1}{2}\underline{\Delta} \cdot \underline{\underline{K}} \cdot \underline{\Delta}, \tag{3}$$

where $\underline{\underline{K}}$ is the symmetric stiffness matrix,

$$\underline{\underline{K}} = \begin{pmatrix} K_{\xi\xi} & K_{\xi\eta} & K_{\xi\varsigma} & K_{\xi\theta} & K_{\xi\phi} & K_{\xi\psi} \\ & K_{\eta\eta} & K_{\eta\varsigma} & K_{\eta\theta} & K_{\eta\phi} & K_{\eta\psi} \\ & & K_{\varsigma\varsigma} & K_{\varsigma\theta} & K_{\varsigma\phi} & K_{\varsigma\psi} \\ & & & K_{\theta\theta} & K_{\theta\phi} & K_{\theta\psi} \\ & & & & K_{\phi\phi} & K_{\phi\psi} \\ & & & & & K_{\psi\psi} \end{pmatrix}, \tag{4}$$

with $\Delta = (\xi, \eta, \varsigma, \theta, \phi, \psi)$ which contains, respectively, the float's spatial and angular displacements with respect to the bearing in a cartesian coordinate system. The components of the forces and torques, $\underline{F}$, can be calculated using virtual work arguments in the usual way,

$$\underline{F} = -\underline{\underline{K}}\,\underline{\Delta}. \tag{5}$$

Initially we will concentrate on the equations of motion in a plane perpendicular to Earth's gravity. With reference to equation (2), we can take moments about the centre of buoyancy and use subscripts to denote the cartesian components of torque and force,

$$\Gamma_z = \Delta x F_y - \Delta y F_x, \tag{6}$$

where $(\Delta x, \Delta y)$ is the location of the centre of mass with respect to the centre of buoyancy.

Equation (5) can then be written for three degrees of freedom, ξ, η and angular motion, ψ about the z axis,

$$\begin{pmatrix} F_x \\ F_y \\ \Gamma_z \end{pmatrix} = -\begin{pmatrix} K_{\xi\xi} & K_{\xi\eta} & K_{\xi\psi} \\ K_{\xi\eta} & K_{\eta\eta} & K_{\eta\psi} \\ K_{\xi\psi} & K_{\eta\psi} & K_{\psi\psi} \end{pmatrix} \begin{pmatrix} \xi \\ \eta \\ \psi \end{pmatrix}. \tag{7}$$

Substituting (6) into (7) and solving for ψ, we find

$$\psi = -\left(K_{31}^{-1} - \Delta y K_{33}^{-1}\right) F_x - \left(K_{32}^{-1} + \Delta x K_{33}^{-1}\right) F_y, \tag{8}$$

where K_{33}^{-1}, for example, is a component of the inverse matrix of $\underline{\underline{K}}$. Setting $\psi = 0$, we find

$$\begin{aligned} 0 = &\left(K_{\eta\eta}K_{\xi\psi} - K_{\xi\eta}k_{\eta\psi} - \Delta y\left(-K_{\xi\xi}K_{\eta\eta} + K_{\xi\eta}^2\right)\right) F_x \\ &+ \left(K_{\xi\xi}K_{\eta\psi} - K_{\xi\psi}K_{\xi\eta} + \Delta x\left(-K_{\xi\xi}K_{\eta\eta} + K_{\xi\eta}^2\right)\right) F_y. \end{aligned} \tag{9}$$

We are looking for the conditions on the stiffnesses that ensure that the rotation angle, ψ, is zero irrespective of the magnitudes of the forces. This gives us two equations which the stiffnesses have to satisfy in terms of the coordinates of the applied force,

$$\Delta x = \frac{K_{\xi\xi}K_{\eta\psi} - K_{\xi\eta}K_{\xi\psi}}{K_{\xi\xi}K_{\eta\eta} - K_{\xi\eta}^2}, \tag{10}$$

and

$$\Delta y = \frac{K_{\xi\eta}K_{\eta\psi} - K_{\eta\eta}K_{\xi\psi}}{K_{\xi\xi}K_{\eta\eta} - K_{\xi\eta}^2}. \tag{11}$$

These equations indicate that, in principle, we can tune the suspension characteristics to eliminate the coupling of the applied force to rotation. Given that inertial accelerations will act at the COM of the levitated object and that the COM will in general not be located at centre of buoyancy, tuning the stiffnesses in accordance with equations (10) and (11) will decouple the measurement degree of freedom of the device from ground vibrations. We note that the cross-coupling terms, such as K_{xy}, can normally be made significantly smaller than terms such as K_{xx} simply by reasonable manufacturing tolerances. Hence if we wish the centre of buoyancy to correspond to the centre of mass, the stiffnesses must satisfy the following relationships,

$$\frac{K_{\eta\psi}}{K_{\eta\eta}} \approx \Delta x, \tag{12}$$

and

$$\frac{K_{\xi\psi}}{K_{\xi\xi}} \approx -\Delta y. \tag{13}$$

3. Tuning the rotational period of the float

3.1. Modelling the rotational stiffness due to one spring element

The aim of this section is to show that the rotational stiffness of the float can be tuned by changing the relative stiffnesses and forces applied by individual spring elements that are appropriately positioned. In general a spring element located at a point, say x_0 on the bearing, will be stretched by a rotation of the float about its centre, as shown in Fig. 2. In what follows we will ignore the linear displacement of the float relative to the bearing and we define the length of the spring, g, in Fig. 2, as being the distance between the point on the bearing where the spring is attached and a point on the float measured perpendicular to the bearing surface. This of course is not an accurate way of modelling a real spring, however this model is convenient and adequate when considering the superconducting magnetic and electrostatic suspensions described below. We can clearly store energy in the spring by changing its length. However we will also suppose that we can store energy by a simple rotation of the surface facing the actuator, with no change in gap. If we define the energy stored in an individual spring as ε, we can therefore define two stiffnesses as follows:

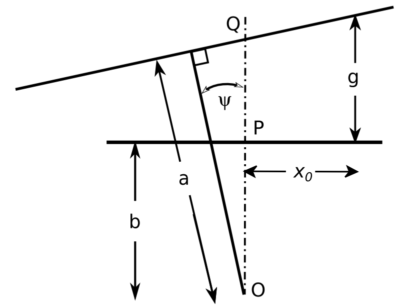

Fig. 2. Schematic diagram showing the construction and parameters required to calculate the gap between the inner surface of the float and bearing (see equation (16)).

$$k_{\psi\psi} = \left[\frac{d^2\varepsilon\left(\psi, g = const\right)}{d\psi^2}\right]_{\psi=0} \tag{14}$$

and

$$k_{\psi\psi}^{x_0} = \left[\frac{d^2\epsilon\left(g\left(\psi\right)\right)}{d\psi^2}\right]_{\psi=0}. \tag{15}$$

Fig. 2 shows a schematic diagram of the gap, g, at a position x_0, between the bearing and the inner surface of the float for a float rotation of ψ.

The gap can be calculated as a function of the position of the spring with respect to the symmetry axis of the bearing, x_0, and the angular rotation, ψ, using Fig. 2,

$$g\left(\psi\right) = \frac{a}{\cos\psi} - b + x_0 \tan\psi. \tag{16}$$

The rotational stiffness due to the change in the gap as a function of ψ is then

$$k_{\psi\psi}^{x_0} = \frac{d}{d\psi}\left(\frac{d\varepsilon}{dg}\frac{dg}{d\psi}\right) = \frac{d\varepsilon}{dg}\frac{d^2g}{d\psi^2} + \frac{d^2\varepsilon}{dgd\psi}\frac{dg}{d\psi}. \tag{17}$$

Using equation (16) we find

$$k_{\psi\psi}^{x_0} = a\frac{d\varepsilon}{dg} + x_0\frac{d^2\varepsilon}{dgd\psi}. \tag{18}$$

The total stiffness of the ith spring against rotation is the sum of the two spring constants given in equations (14) and (15),

$$K_{\psi\psi}^{i} = k_{\psi\psi} + a\frac{d\varepsilon}{dg} + x_0\frac{d^2\varepsilon}{dgd\psi}. \tag{19}$$

We see that the contribution that an individual spring has to the total stiffness of the float depends on how the energy varies with the gap and the tilt angle but also on its position relative to the symmetry axes of the float. In the next section we will show that the rotational stiffness of the float can be tuned, depending on the form of ε, using equation (19).

3.2. Calculation of the stiffness using superconducting diamagnetic and electrostatic suspensions

3.2.1. Modelling of electrostatic suspensions

For an actuator comprising a parallel plate capacitor of capacitance, C, with potential difference, V, the energy stored is equal to

$$\varepsilon = \frac{1}{2}CV^2. \quad (20)$$

However a voltage source must do work δW in order to maintain a constant voltage across the capacitor as the capacitance changes by δC. The work done by the capacitor is equal to

$$\delta W = -\delta C V^2. \quad (21)$$

The net energy of a parallel plate capacitor of gap g and area A can be considered to be therefore

$$\epsilon_e = -\frac{1}{2}\frac{\varepsilon_0 A}{g}V^2, \quad (22)$$

where from equation (16) we have $g = a - b$ for $\psi = 0$. The force due to the simple electrostatic spring when it undergoes an extension is

$$F_e = -\frac{d\varepsilon_e}{dg} = -\frac{1}{2}\frac{C}{g}V^2 \quad (23)$$

and its linear stiffness is

$$k_{gg} = -\frac{C}{g^2}V^2. \quad (24)$$

Notice that the force is negative and the stiffness is negative i.e. the force between the plates is attractive and the stiffness produces an instability. Using equation (16) we can evaluate the stiffness, due to the change in gap, of an electrostatic spring located at position x_0 as illustrated in Fig. 2, as

$$k^{x_0}_{\psi\psi} = k_{gg}\left(x_0^2 - \frac{ga}{2}\right). \quad (25)$$

We can now calculate the change in energy of the electrostatic spring due to pure tilt by supposing, for simplicity, that the electrodes are rectangular and of dimension d in the x direction and h in the z direction (out of the page) in Fig. 2. The capacitance as a function of tilt, ψ, can easily be calculated as,

$$\begin{aligned} C(g,\psi) &\simeq \varepsilon_0 \int_{-d/2}^{+d/2} \frac{h dx}{(g-\psi x)} \\ &= C(g,\psi=0)\cdot\left(1 + \frac{1}{12}\frac{d^2}{g^2}\psi^2 + O\left(\psi^4\right)\right). \end{aligned} \quad (26)$$

We then find that

$$k_{\psi\psi} = \frac{\partial^2\varepsilon}{\partial\psi^2} = -\frac{1}{12}\frac{Cd^2}{g^2}V^2. \quad (27)$$

We can now write the complete stiffness for the electrostatic spring using equation (19),

$$K^i_{\psi\psi} = k_{gg}\left(x_0^2 + \frac{d^2}{12} - \frac{ga}{2}\right). \quad (28)$$

This equation shows that the net stiffness contribution to the float is a function of the position of the spring, the dimensions of the electrode and the geometry of the float and bearing. An electrostatic spring located at finite distance (x_0) relative to the symmetry axis of the float/bearing system will contribute an instability and the finite size of the electrodes also increases the instability of the float/bearing system. On the other hand, if the spring is located on the symmetry axis, the electrostatic stiffness is such as to produce a *positive stiffness*. We note that there are a number of ways that the oscillation period and sensitivity of the suspension can be tuned by varying simple geometrical properties. However, more importantly, the stiffness of the electrostatic spring can be tuned *in situ* by varying the voltages applied to individual spring elements. It is interesting to note that, if we ignore the intrinsic stiffness, $k_{\psi\psi}$ (the second term in the bracket in equation (28)), an electrostatic spring can contribute zero rotational stiffness when

$$x_0 = \sqrt{\left(\frac{ga}{2}\right)}. \quad (29)$$

This is of interest in the case of the superconducting suspension.

3.2.2. Modelling a superconducting magnetic suspension

In the case of a superconducting magnetic spring, the energy dependence of the spring with inductance will depend on whether the inductance is driven in constant current mode or whether a persistent current is stored. In the latter case, if an initial current I_0 is stored when the inductance is equal to L_0, the flux, $\Phi_0 = I_0 L_0$ will be conserved. As the inductance changes with the gap between the magnetic coil and the superconducting surface of the float, the energy will be given by

$$\varepsilon_m = \frac{1}{2}\frac{\Phi_0^2}{L(g)}. \quad (30)$$

In a simple model of a flat 'pancake' coil, with radius considerably larger than the gap between coil and the float, the inductance can, to a good approximation, be taken to be proportional to the volume between the coil and the float [12]. For rotational motion, as defined in Fig. 2, this volume will be proportional simply to the gap, g, and we can then assume that $L = \beta g$, where β is a constant. In this approximation, the potential energy will be equal to

$$\varepsilon_m = \frac{1}{2}\frac{\Phi_0^2}{\beta g}. \quad (31)$$

This also implies that $k_{\psi\psi} = 0$. Using this form of the stored energy the total rotational stiffness of the float can be found using equation (19) to be

$$K^i_{\psi\psi} = k^{x_0}_{\psi\psi} = k_{gg}\left(x_0^2 - \frac{ga}{2}\right), \quad (32)$$

where here we define

$$k_{gg} = \frac{\Phi_0^2}{L_0 g^2}. \quad (33)$$

We see that the rotational stiffness contribution due to the superconducting spring, when it is located on the symmetry axis, produces the opposite sign of stiffness to that of the spring located at distance x_0 away from the axis. This can be understood with reference to Fig. 2: if the pancake coil is located at P, on the symmetry axis of the bearing, rotation, ψ, of the float moves the point of application of its repulsive force on the float to Q. The force is perpendicular to the surface of the float. It should be born in mind that this force acting on the float by the pancake coil is cancelled by a similar coil, not shown in Fig. 2, located on the opposite side of the bearing (a distance $2a$ below P). However the forces from the pairs of coils produce a torque that increases the rotation angle. On the other hand a pancake coil located at x_0 will apply a repulsive force to the float that decreases as ψ increases. This adds stiffness to the rotational mode. Again, in the complete picture, the force due to the coil at x_0 is cancelled by a similar coil located on the opposite face of the bearing that is not shown in Fig. 2. In order to produce a zero stiffness suspension the relationship between the radius of the float, a, the gap, g, and the distance x_0 is identical with that given in equation (29).

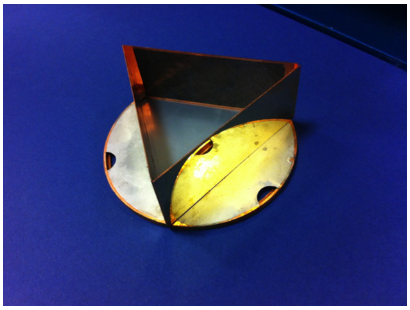

Fig. 3a. Showing the underside of the float.

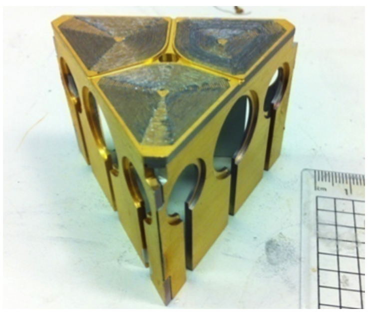

Fig. 3b. Showing the bearing structure with lead lift coils and recesses for the side coils.

4. Status of experimental investigations

We have constructed a torsion balance that implements the techniques described in this paper that is based on superconducting actuators. Figs. 3a and 3b show photographs of the new torsion balance which has three-fold symmetry and is designed for operation in the lab (not space). The float (Fig. 3a) is manufactured from copper panels with an interior coating of lead. The exterior of the side panels of the float are gold coated to allow the angular displacement to be measured optically. The bearing is shown in Fig. 3b. There are three levitation coils on the top surface of the bearing that provide lift and vertical stability. On each vertical side of the bearing there are three coils (not in place in Fig. 3b): one coil sits at the centre of each panel and provides transverse stability and rotational instability ('instability' coil); at each extremity of each side panel there are coils that provide predominantly rotational stiffness ('stability' coil). The coils are made from lead and are designed to work in persistent current mode.

A procedure can be defined that tunes the rotational stiffness and the centre of buoyancy such that the net force and torque on the float are zero. We also need to define independently a transverse stiffness that gives the float stability against horizontal motion. We will briefly outline this process here in a qualitative way using the simple case of the rectangular float shown in Fig. 1, assuming that we replace the mechanical springs with superconducting actuators. Firstly we can use equations (16) and (30) to find the off-diagonal stiffness term for a single coil that is relevant for the tuning of the centre of buoyancy in the y direction, vertically up the in Fig. 1 (see equation (13)),

$$K^i_{\xi\psi} = \frac{\Phi_i^2}{L_0 g^2} y_0, \tag{34}$$

where we have assumed $\psi = 0$ and where y_0 (rather than x_0) is now the distance of the coil from the symmetry axis located at $y = 0$. The centre of buoyancy can be adjusted by introducing a difference between the fluxes, Φ_A and Φ_B, in the coils labelled A_1 and B_1 located at $\pm y_0$ in Fig. 1. The net change in the off-diagonal stiffness becomes

$$K_{\xi\psi} = \frac{y_0}{L_0 g^2}\left(\Phi_B^2 - \Phi_A^2\right). \tag{35}$$

In order to maintain zero torque on the float during this process we need to modify the fluxes in coils A_2 and B_2 in a similar way. Balancing the torques due to opposed actuators allows us to consider the tuning procedure in terms of only the three coils on a single side of the float (note that the instability coils are not indicated in Fig. 1). This gives us three conditions: the difference in the stiffnesses of the stability coils, the difference between the stiffnesses of the stability coils and the instability coil and the sum of the stiffnesses of all coils. These conditions are given in terms of the centre of buoyancy correction, the rotational period and the transverse stiffness, respectively. As we have three unknowns in terms of the fluxes in each coil, we can satisfy these conditions.

We have performed experiments in order to demonstrate the adjustment of rotational stiffness through balancing 'stabilising' and 'destabilising' springs using a simplified version of the triangular superconducting torsion balance. The three central 'instability' coils were connected in series, as were three 'stability' coils that would act to push the float, say, in a clockwise direction and the other three stability coils that would drive the float in the anticlockwise direction, giving four independent circuits when the levitation coils are included. This was sufficient to allow the angular stiffness to be adjusted, but not to carry out the 'centre of buoyancy' adjustments. The float in this case was made of folded niobium sheet which was lighter than the float shown in the Fig. 3a, and could be levitated with a smaller current but was, however, difficult to manufacture accurately. The angular displacement of the float was measured using the persistent currents stored in the bearing using an inductance readout. A torque could be applied to the float by an additional coil facing the float from the outside.

The angular stiffness, as measured directly by the angular displacement produced by a given torque applied by the external coil, was measured for a number of different configurations of current in the side coils. All configurations were expected to give about the same stiffness for transverse displacements, but should have given different angular stiffness due to the relative strength of the unstable and the stable magnetic springs. The measured angular stiffnesses are tabulated in Table 1, alongside the predicted value from our model. It can be seen that the results are approximately as predicted and we take them to show that the model described in Section 3 above is viable and that it is indeed possible to create instability in the float with stable magnetic springs.

Table 1
Summary of results of a preliminary experiment to show that the angular stiffness of the superconducting levitation system can be reduced by changing the ratios of currents flowing through the coils at the centres and ends of the side panels of the bearing shown in Fig. 3b.

Measured angular stiffness μNm/rad	Calculated angular stiffness μNm/rad
67 ± 13	60
38.5 ± 7	28
18.8 ± 2	11.2
6.5 ± 1.6	4.4

These early experiments were promising but could not satisfactorily explore low values of stiffness and we believe that this was because the torsion balance, perhaps due to its imperfect geometry, would find local minima in its potential energy as the stiffness was reduced. We are now working toward using the float shown in Fig. 3a together with a servo controller to more thoroughly explore the ideas described in this paper and will report the results in a future publication.

5. Discussion

This paper is aimed at illustrating the concepts and indicating approximate solutions to the problems associated with linear to rotational coupling and achieving low rotational stiffness. Clearly more detailed paper studies, taking into consideration the non-linearities of the 'springs', edge effects, imperfections in the geometry of the float etc, could be made using finite element methods. We have assumed that bias forces and stiffnesses can be added without the addition of noise to the torsion balance and, in principle, this is not possible. For example, there will be fluctuations in the magnitude of the potentials applied to an electrostatic suspension that, at some level, couple to its rotational mode. However these problems are well understood as there has been a lot of work done recently on electrostatic accelerometers for linear motion for space-based gravitational wave detectors [2] and for testing the Equivalence Principle [14]. Superconducting suspensions are passive in persistent mode and can therefore be completely decoupled from external current supplies. The effective inductance of the pancake coils depends on the penetration depth of the superconducting material [12] which is temperature dependent and this will lead to fluctuations in the magnetic forces and torques applied to the float. Clearly more experimental investigations need to be performed in order to realise a high quality device.

6. Conclusions

We have presented a simple analysis of the static characteristics of a torsion balance that is suspended using electrostatic or superconducting magnetic actuators. We have shown that it is possible for such a device to be insensitive to linear accelerations provided that the stiffnesses defining its static stability can be adjusted appropriately. Using analytical expressions for electrostatic and superconducting 'springs' we have shown that the magnitude and sign of their rotational stiffnesses can be modified using the geometry of the suspended object. In particular, in principle, a zero stiffness can be achieved in both cases by an appropriate choice of the gap relative to the float dimensions and the location of the 'spring' relative to the symmetry axis of the float. Importantly these adjustments can be realised when the torsion balance is operational, even in a cryogenic environment for example, by adjusting the voltage on an electrode or the current in a coil.

We have shown results of a preliminary experiment that supports the idea that the rotational stiffness can be tuned in the way we describe. We suggest that, by using the principles we describe here, it should be possible to construct devices that measure torques with low stiffness and low sensitivity to ground vibration and hence mimic the characteristics of the Cavendish torsion balance. We would emphasise that the motivation for this work is not to necessarily to improve the quality of existing Cavendish torsion balances per se but to develop devices that will enable searches for putative forces with ranges of less than 50 μm or so, which seems to be the current limit of the capability of torsion balances with fibre suspensions of finite length. Finally it is possible to conceive of hybrid torsion balances where the majority of the weight of the suspended 'float' is supported by a mechanical component of non-ideal geometry, a fibre, but the properties of the assembly may be tuned, by the principles discussed here, to achieve an acceptable performance.

Acknowledgements

We are grateful to UK STFC (grant number ST/F00673X/1) who initially supported this work. We are very grateful to Leverhulme Trust (grant number RPG-2012-674) for financial support. We would like to thank Stuart Aston, Eleanor Chalkley, Michaela Nelson for their contribution to the realisation of this project in its earlier stages. This work could not be carried out without the support of our workshop under Stephen Brookes and technical support from David Hoyland and John Bryant. We thank Conner Gettings for many helpful comments on the draft of the paper.

References

[1] E.G. Adelberger, J.H. Gundlach, B.R. Heckel, S. Hoedl, S. Schlamminger, Torsion balance experiments: a low-energy frontier of particle physics, in: A. Faesssler (Ed.), Prog. Part. Nucl. Phys. 62 (1) (2009) 102–134.

[2] M. Armano, H. Audley, G. Auger, J.T. Baird, P. Binetruy, M. Born, D. Bortoluzzi, N. Brandt, A. Bursi, M. Caleno, A. Cavalleri, A. Cesarini, M. Cruise, K. Danzmann, M. de Deus Silva, I. Diepholz, R. Dolesi, N. Dunbar, L. Ferraioli, V. Ferroni, E.D. Fitzsimons, R. Flatscher, M. Freschi, J. Gallegos, C. Garcia Marirrodriga, R. Gerndt, L. Gesa, F. Gibert, D. Giardini, R. Giusteri, C. Grimani, J. Grzymisch, I. Harrison, G. Heinzel, M. Hewitson, D. Hollington, M. Hueller, J. Huesler, H. Inchauspe, O. Jennrich, P. Jetzer, B. Johlander, N. Karnesis, B. Kaune, C.J. Killow, N. Korsakova, I. Lloro, L. Liu, J.P. Lopez-Zaragoza, R. Maarschalkerweerd, S. Madden, D. Mance, V. Martin, L. Martin-Polo, J. Martino, F. Martin-Porqueras, I. Mateos, P.W. McNamara, J. Mendes, L. Mendes, A. Moroni, M. Nofrarias, S. Paczkowski, M. Perreur-Lloyd, A. Petiteau, P. Pivato, E. Plagnol, P. Prat, U. Ragnit, J. Ramos-Castro, J. Reiche, J.A. Romera Perez, D.I. Robertson, H. Rozemeijer, F. Rivas, G. Russano, P. Sarra, A. Schleicher, J. Slutsky, C. Sopuerta, T.J. Sumner, D. Texier, J.I. Thorpe, C. Trenkel, D. Vetrugno, S. Vitale, G. Wanner, H. Ward, P.J. Wass, D. Wealthy, W.J. Weber, A. Wittchen, C. Zanoni, T. Ziegler, P. Zweifel, Charge-induced force noise on free-falling test masses: results from LISA Pathfinder, Phys. Rev. Lett. 118 (17) (2017).

[3] H. Cavendish, Experiments to determine the density of the Earth, Philos. Trans. R. Soc. Lond. 88 (5–6) (1798) 469–526.

[4] H.A. Chan, M.V. Moody, H.J. Paik, Superconducting gravity gradiometer for sensitive gravity measurements. 2. Experiment, Phys. Rev. D 35 (12) (1987) 3572–3597.

[5] G.T. Gillies, R.C. Ritter, Torsion balances, torsion pendulums and related devices, Rev. Sci. Instrum. 64 (2) (1993) 283–309.

[6] Giles D. Hammond, Clive C. Speake, Christian Trenkel, Antonio Pulido Paton, New constraints on short-range forces coupling mass to intrinsic spin, Phys. Rev. Lett. 98 (8) (2007).

[7] J. Jin, T. Higuchi, M. Kanemoto, Electrostatic levitator for hard-disk media, IEEE Trans. Ind. Electron. 42 (5) (1995) 467–473.

[8] G.M. Keiser, J.E. Faller, New approach to the Eotvos experiment, Bull. Am. Phys. Soc. 24 (1979) 579.

[9] W.A. Koldewyn, J.E. Faller, New method of measuring gravitational constant, Bull. Am. Phys. Soc. 17 (1972) 472.

[10] S.K. Lamoreaux, The Casimir force: background, experiments, and applications, Rep. Prog. Phys. 68 (1) (2005) 201–236.

[11] Jiro Murata, Saki Tanaka, A review of short-range gravity experiments in the LHC era, Class. Quantum Gravity 32 (3) (2015).

[12] H.J. Paik, Superconducting tunable-diaphragm transducer for sensitive acceleration measurements, J. Appl. Phys. 47 (3) (1976) 1168–1178.

[13] T.J. Quinn, C.C. Speake, R.S. Davis, Novel torsion balance for the measurement of the Newtonian gravitational constant, Metrologia 34 (3) (1997) 245–249.

[14] Pierre Touboul, Gilles Metris, Manuel Rodrigues, Yves Andre, Quentin Baghi, Joel Berge, Damien Boulanger, Stefanie Bremer, Patrice Carle, Ratana Chhun, Bruno Christophe, Valerio Cipolla, Thibault Damour, Pascale Danto, Hansjoerg Dittus, Pierre Fayet, Bernard Foulon, Claude Gageant, Pierre-Yves Guidotti, Daniel Hagedorn, Emilie Hardy, Phuong-Anh Huynh, Henri Inchauspe, Patrick Kayser, Stephanie Lala, Claus Laemmerzahl, Vincent Lebat, Pierre Leseur, Francoise Liorzou, Meike List, Frank Loeffler, Isabelle Panet, Benjamin Pouilloux, Pascal Prieur, Alexandre Rebray, Serge Reynaud, Benny Rievers, Alain Robert, Hanns Selig, Laura Serron, Timothy Sumner, Nicolas Tanguy, Pieter Visser, Microscope mission: first results of a space test of the equivalence principle, Phys. Rev. Lett. 119 (23) (2017).

[15] T.A. Wagner, S. Schlamminger, J.H. Gundlach, E.G. Adelberger, Torsion-balance tests of the weak equivalence principle, Class. Quantum Gravity 29 (18) (2012).

[16] E. Willemenot, P. Touboul, Electrostatically suspended torsion pendulum, Rev. Sci. Instrum. 71 (1) (2000) 310–314.